IOSR Journal of Applied Geology and Geophysics (IOSR-JAGG)
e-ISSN: 2321–0990, p-ISSN: 2321–0982. Volume 14, Issue 4 Ser. 1 (July – August 2026), PP 31-39
www.iosrjournals.org

Amplitude Variation With Offset (AVO) Analysis For Lithology And Fluid Characterisation Of The Heimdal Formation Reservoir, Northern North Sea

M. Bello, G. Mohammed, M. A. Yusuf And Y. Abdulmumin
Department Of Physics, Abubakar Tafawa Balewa University, Bauchi – Nigeria
Department Of Geology, Abubakar Tafawa Balewa University, Bauchi – Nigeria

Abstract

This study applies AVO analysis to the Paleogene Heimdal Formation reservoir in the northern North Sea to predict lithology, pore fluids and seismic properties at interfaces in the Heimdal Formation sands. The study integrates well-log data, prestack Common Depth Point (CDP) gathers, and rock physics analysis to evaluate elastic property contrasts across key reservoir interfaces. AVO modelling was performed using Shuey's approximation, while intercept-gradient analysis, elastic contrast analysis, and supergather enhancement were employed to improve the interpretation of seismic amplitude responses. The results show that the interface between silty shale and unconsolidated clean sand exhibits very weak amplitude anomalies because of low acoustic and shear impedance contrasts of respective values of -0.027 and 0.063, making seismic detection of these reservoir intervals challenging. In contrast, the shale–cemented sandstone interface displays stronger amplitude variations resulting from higher elastic impedance contrasts associated with early cementation. Intercept-gradient cross-plots and AVO attribute volumes further demonstrate the capability of AVO attributes to distinguish lithological variations and identify reservoir heterogeneity within the Heimdal Formation. In the block model AVO two intervals of the clean sands (cemented and unconsolidated clean sand) were considered. The clean sand is characterised as an oil filled sand, it exhibits a lower negative intercept and a negative gradient (AVO class 2), while the cemented sand characterise as brine filled sand exhibits a higher positive intercept and a higher positive gradient (AVO class 1).

Keywords: *Amplitude Variation with Offset (AVO); Heimdal Formation; Northern North Sea; Rock Physics; Elastic Impedance; Reservoir Characterization; Pre-stack Seismic Analysis*

Date of Submission: 01-07-2026 Date of Acceptance: 10-07-2026

I. Introduction

Amplitude Variation with Offset (AVO) analysis is one of the most widely applied prestack seismic interpretation techniques for reservoir characterization because it exploits changes in seismic reflection amplitudes with incidence angle to infer lithology, pore-fluid distribution, and rock elastic properties (Shuey, 1985; Rutherford and Williams, 1989). Unlike conventional stacked seismic data, which primarily provide structural information, AVO analysis preserves offset-dependent amplitude variations that are sensitive to contrasts in compressional-wave velocity (Vp), shear-wave velocity (Vs), and density across geological interfaces. Consequently, AVO has become an indispensable tool for hydrocarbon exploration, prospect evaluation, and reservoir monitoring in clastic petroleum systems.

Deep-marine Paleogene reservoirs of the northern North Sea contain some of the most prolific hydrocarbon accumulations in Europe. Among these reservoirs, the Heimdal Formation consists of laterally discontinuous turbidite sandstones interbedded with marine shales, producing complex seismic responses because of rapid lithological changes and thin-bed interference (Avseth et al., 2001b). Conventional post-stack seismic interpretation alone often fails to distinguish hydrocarbon-bearing sands from surrounding shales, particularly where impedance contrasts are weak. Consequently, AVO analysis provides an effective approach for reducing exploration uncertainty and improving reservoir prediction (Avseth et al., 2001a).

II. Geological Setting

The Heimdal Formation belongs to the Paleocene Lista Formation and forms an important deep-water turbidite reservoir deposited during periods of rapid basin subsidence and sediment gravity-flow activity in the northern North Sea (Figure 1). Sand deposition occurred through submarine channelized and unconfined gravity flows sourced primarily from the Scottish Highlands and Shetland Platform (Cayley, 1987). Individual reservoir bodies are generally 10–30 m thick and are separated by marine shale units that create complex stratigraphic trapping conditions (Ahmadi et al., 2003)(Figure 2).

The reservoir interval investigated in this study occurs between approximately 2153 and 2183 m measured depth and consists of stacked sandstone bodies interbedded with shale (Whyatt et al., 1992; Avseth et al., 2001a; Avseth et al., 2005). These thinly bedded successions produce subtle impedance contrasts that make conventional seismic interpretation challenging but are well suited for prestack AVO investigation.

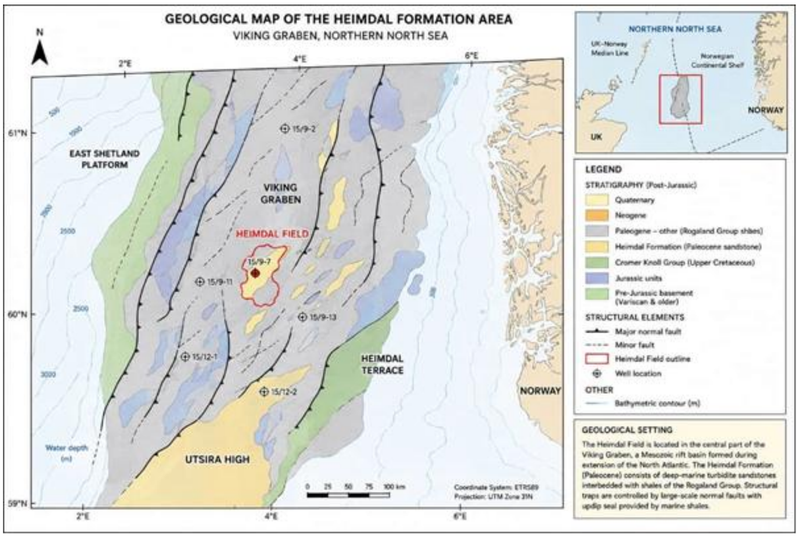

The Heimdal Field is located in the central part of the Viking Graben, a Mesozoic rift basin formed during extension of the North Atlantic. The Heimdal Formation (Paleocene) consists of deep-marine turbidite sandstones interbedded with shales of the Rogaland Group. Structural traps are controlled by large-scale normal faults with updip seal provided by marine shales.

Figure 1. Regional geological map of the northern North Sea showing the location of the Heimdal Formation reservoir (Ahmadi et al., 2003).

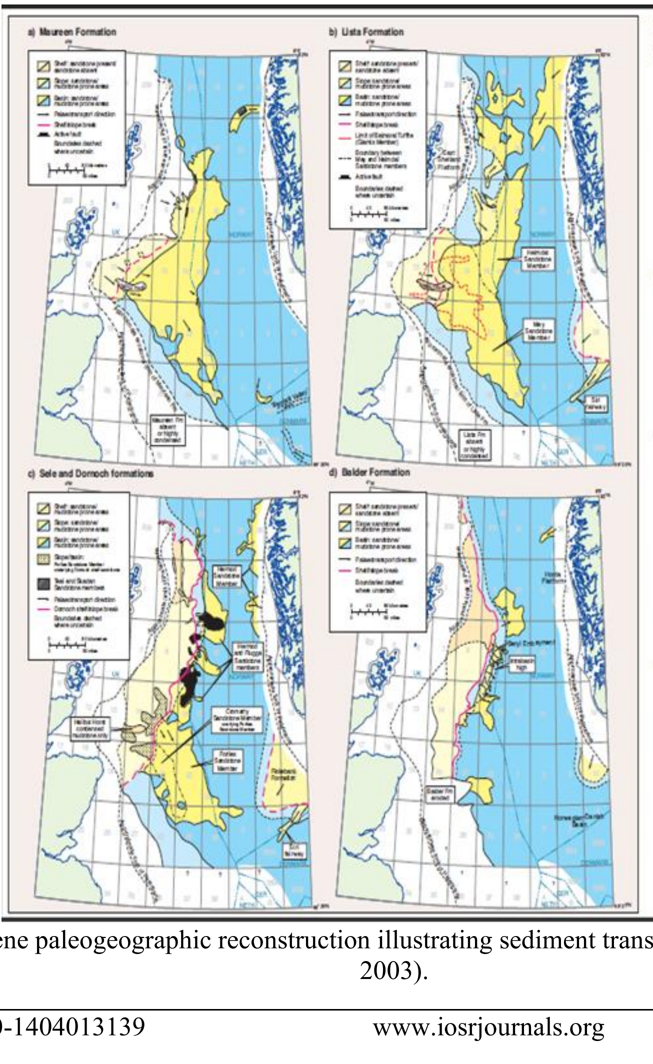

Figure 14.9
Palaeogeographic maps of the Paleocene.
a) Maureen Formation times.
The primary depocentre extended from the Outer Moray Firth Basin to the Central Graben, with an additional depocentre created in the hanging wall of the fault bounding the East Shetland Platform in UK Quadrant 9. The sand-prone shelf and slope areas are restricted to the Outer Moray Firth Basin and the southern and south-eastern margins of the East Shetland Platform; these areas were the primary sources for sand input into the deeper basin. See section 2.2.1 for discussion.
b) Lista Formation times.
Sandstone units are developed extensively in the Outer Moray Firth Basin to Central Graben area, and over the Viking Graben. For the first time during the Paleocene, sand was also supplied into the East Shetland Basin where a major depocentre was created in the hanging wall of the fault bounding the East Shetland Platform. See section 2.2.2 for discussion.
c) Sele and Dornoch formation times.
The Dornoch Formation is composed of shelfal or deltaic sediments, whereas the Sele Formation contains time-equivalent sandstones and organic-rich hemipelagic sediments deposited in deeper-water and more-distal areas of the North Sea Basin. The development of restricted depocentres, and the recognition of at least four distinct sandstone members in the Sele Formation, suggests that sand deposition became more localised at this time. See section 2.3.1 for discussion.
d) Balder Formation times.
A major transgression resulted in widespread shale deposition. Coastal-deltaic sandstones of the Beauly Member occur in the Outer Moray Firth Basin and extend across the southern East Shetland Platform. These localities were the primary source areas for minor gravity flows that transported sand into the Central and Viking grabens. Additional minor sand fairways existed on the northern Horda Platform and on the margin of the Norwegian-Danish Basin. Odin Member sandstones are developed locally in parts of the Viking Graben and Beryl Embayment. See section 2.3.2 for discussion.

Figure 2: Paleocene paleogeographic reconstruction illustrating sediment transport pathways (Ahmadi et al., 2003).

Reservoir Characteristics

The reservoir interval investigated comprises several lithofacies, including unconsolidated clean sandstone, cemented sandstone, silty sandstone, silty shale, laminated shale, and pure shale (Avseth et al., 2001b). These lithologies differ significantly in porosity, clay content, cementation, and elastic properties, producing contrasting seismic responses.

Well-log analysis indicates that unconsolidated sandstones possess relatively high porosity and low acoustic impedance, whereas cemented sandstones exhibit increased seismic velocities and higher impedance due to quartz cementation (Castagna and Backus, 2000). Shale-rich intervals are characterized by elevated gamma-ray values, higher Vp/Vs ratios, and lower shear rigidity. These variations directly influence reflection amplitudes observed on prestack seismic data (Castagna and Backus, 2000).

The reservoir occurs at approximately 2.1–2.3 km depth under average reservoir conditions of about 20 MPa effective pressure and 70°C. The principal pore fluids are formation brine and oil, whose contrasting bulk moduli and densities significantly influence the elastic properties of the reservoir rocks (Avseth et al., 2005).

Previous Studies

Several authors have investigated AVO behaviour in North Sea Paleogene reservoirs. Early work demonstrated that combining well-log analysis, statistical rock physics, and prestack seismic inversion enables probabilistic prediction of lithofacies and pore fluids from AVO attributes (Avseth et al., 2001b). Subsequent studies showed that thin turbidite sandstones similar to the Heimdal Formation could be effectively characterized through integrated petrophysical analysis, fluid substitution, and AVO modelling (Eisssa et al., 2009). These studies also highlighted the influence of cementation on elastic properties and confirmed that log-derived rock physics models provide reliable predictions of prestack seismic responses. This study is the first to integrate blocky model AVO and 2D AVO analysis to predict reservoir properties

III. Materials And Methods

Study Area and Dataset

The dataset employed in this study was adapted from the North Sea reservoir characterization dataset described by Avseth et al. 2005 and comprised well logs, petrophysical information, prestack Common Depth Point (CDP) gathers, near- and far-offset partial-stack seismic volumes, and rock physics modelling codes. These datasets provided the basis for quantitative AVO modelling and interpretation.

The well data comprises of five exploration wells containing compressional-wave velocity (Vp), bulk density (RHOB), gamma-ray (GR), neutron porosity (NPHI), and shear-wave velocity (Vs) logs. Corrected density and lithofacies logs for the reference well (Well 2). Two-dimensional prestack CDP gathers. Three-dimensional true-amplitude-preserved near- and far-offset migrated seismic volumes. Well 2 was selected as the reference well because it contains the most complete suite of petrophysical and elastic logs required for AVO analysis.

Well Log Analysis

The first task here was well-log conditioning, which involved verification of sonic, density, gamma-ray, and shear-wave logs. Acoustic impedance (AI) was calculated as: where (Vp) is compressional-wave velocity and (RHOB) is bulk density. Porosity was estimated from density logs, while shale volume was computed from gamma-ray measurements. Where shear-wave logs were unavailable, Vs was predicted using the Greenberg–Castagna empirical relationship after calibration with measured data from the reference well. This procedure ensured reliable estimation of elastic parameters required for AVO modelling.

Principles of Amplitude Variation with Offset (AVO)

Amplitude Variation with Offset (AVO) describes the systematic change in seismic reflection amplitude with increasing source-receiver offset or incidence angle (Rutherford and Williams, 1989). Unlike conventional stacked seismic data, which preserve only zero-offset amplitudes, prestack seismic gathers retain angular information that is sensitive to changes in lithology, porosity, pore-fluid type, and elastic properties.

The theoretical basis of AVO is provided by the Zoeppritz equations, which describe the partitioning of seismic energy at an interface separating two elastic media (Detailed descriptions of the equations and their solutions can be found in Castagna et al., (1999)). Because the complete Zoeppritz equations are computationally complex, practical AVO analysis commonly employs linear approximations developed by Aki and Richards (1980) and later simplified by Shuey (1985) for incidence angles less than approximately 30°.

Under Shuey's approximation, the reflection coefficient is expressed in terms of the AVO intercept and gradient. The intercept primarily reflects contrasts in acoustic impedance across an interface, while the gradient is influenced by changes in Poisson's ratio, shear-wave velocity, and density. Consequently, the intercept is generally associated with lithological contrasts, whereas the gradient provides valuable information regarding pore-fluid variations.

$$R(\theta) \approx R(0) + G.\sin^2\theta \quad 1$$

where

$$R(0) = \frac{1}{2}\left(\frac{\Delta V_p}{V_p} + \frac{\Delta\rho}{\rho}\right) \quad 2$$

and

$$G = \frac{1}{2}\left(\frac{\Delta V_p}{V_p}\right) - 2\frac{V_s^2}{V_p^2}\left(\frac{\Delta\rho}{\rho} + 2\frac{\Delta V_s}{V_s}\right) \quad 3$$

$R(0)$ is define as the zero-offset or normal incidence reflection coefficient, and G is the AVO gradient. While V_p, V_s, and ρ are the average *P*-wave velocity, *S*-wave velocity, and bulk density of the layers, respectively, and ΔV_p, ΔV_s, and $\Delta\rho$ are contrast of the quantities between the two layers. Therefore, $R(0)$ is controlled by contrast in acoustic impedance at the interface, whereas G is controlled by change in V_p and density across the interface as well as change in V_p/V_s ratio. However, the technique suffered from ambiguities caused by lithology effects, overburden effects, tuning effect and sometimes processing and acquisition effect could cause false AVO anomalies (Rutherford and Williams, 1989). Use of simple geologic models and lack of s-wave velocity information are common reasons for failure.

In practice, if amplitudes picked along a move-out corrected event on a CMP gather are plotted against $\sin^2\Theta$, they can be fitted to a straight line. The slope of the line gives the AVO gradient attribute and the ordinate at intercept gives the AVO intercept attribute. The AVO gradient is directly related to the change in Poisson ratio, which in turn is directly related to fluid saturation in reservoir rock (Castagna and Backus, 2000). The AVO intercept attribute, in lieu of conventional stack can be used to derive acoustic impedance attribute, which is directly related to porosity in reservoir rocks.

The pattern with which amplitude vary with offset depends on the combination of reservoir rock and fluid properties. Detection of a pattern is dictated primarily by the signal to noise ratio and the range of incidence angle that is spanned by the offset range of CMP gather for a target horizon. The shallower the reflector the wider the range of incidence angle; hence, AVO indicators are best determined for shallow targets (Avseth et al., 2001a).

Seismic Data Analysis

True-amplitude-preserved prestack CDP gathers were analysed using Hampson–Russell STRATA software. Near- and far-offset partial stacks were examined to assess offset-dependent amplitude variations across the Heimdal reservoir interval. Supergather generation was performed to improve signal-to-noise ratio before AVO interpretation. Reflection amplitudes were extracted at selected reservoir horizons, and amplitude-versus-angle plots were generated to identify characteristic AVO responses associated with sandstone and shale interfaces (Rutherford and Williams, 1989).

IV. Results And Discussion

Blocky Model AVO

A quick first look technique called blocky AVO was used to differentiate oil to brine in the well log data. This technique uses average values over intervals to see the potential effects of hydrocarbon on reflectivity at the top of reservoir interface (Figure 3). For each interface, the expected AVO response at the target depth is calculated using Shuey's approximation of the Zoeppritz equation. A near and far stack angles of 8 and 26 degrees were used respectively. Two intervals of the clean sands (cemented and unconsolidated clean sand) were considered. The clean sand is characterised as an oil filled sand, it exhibits a lower negative intercept and a negative gradient (AVO class 2), while the cemented sand characterise as brine filled sand exhibits a higher positive intercept and a higher positive gradient (AVO class 1); these plots are shown in Figure 3.

It is worthy to note the contrast in properties at the interface silty shale on clean sand; the acoustic impedance contrast is small and negative (-0.027) indicating that the underlying clean sand has lower acoustic impedance compared to the silty-shale. The shear impedance contrast is also comparatively small (0.063). It is obvious that reflectivity of this interface will be very small. The elastic impedance contrast at this interface appears to be also high (-0.414 at 26^0), this is because Vp/Vs information is not lost. However, the shale on cemented sand interface has reasonable contrast in all the elastic properties. This can be explained by cemented rocks have higher seismic properties than shale due to its better connectivity and contacts among the grains.

Figure 4 and 5 are the AI, EI and SI contrast analyser showing some of the elastic properties calculated from the averages. Specifically, this shows the contrast in acoustic impedance (AI), shear Impedance (SI), and elastic impedance (EI) between the upper and lower lithologies defining the two interfaces interface. For example the contrast in AI for interface silty shale on clean sand is given by:

$$AI_{contrast} = \frac{(AI_{clean\ sand} - AI_{silty\ sahle})}{(AI_{clean\ sand} + AI_{silty\ sahle})} \quad 4$$

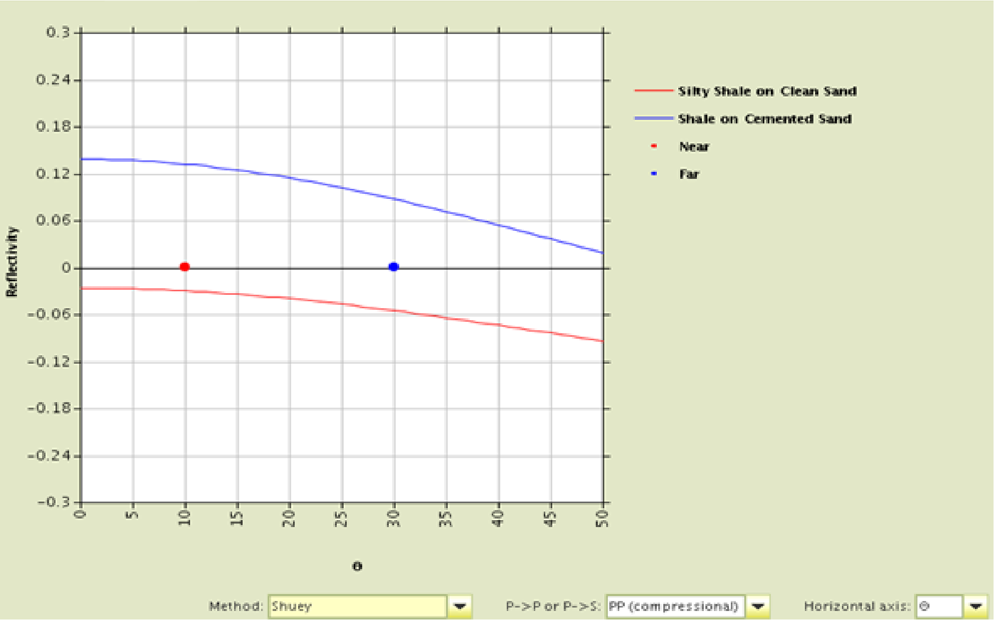

Method: Shuey
P->P or P->S: PP (compressional)
Horizontal axis: θ

Figure 3. Reflectivity versus angle plot for clean sands capped by silty-shale and cemented sandstone capped by shale.

It can be seen that the acoustic impedance contrast at both the interfaces is small and negative indicating that the underlying clean sand has slightly lower acoustic impedance compared to the overlying silty-shale, while the cemented sand has higher acoustic impedance than the overlying shale.

Deterministic AVO analysis of CDP gathers

Hampson Russell's AVO was used to carry out a 2-D AVO analysis on a 2D line of NMO -corrected pre-stack CDP gathers which passes through well 2 corresponding to CDP 2232,

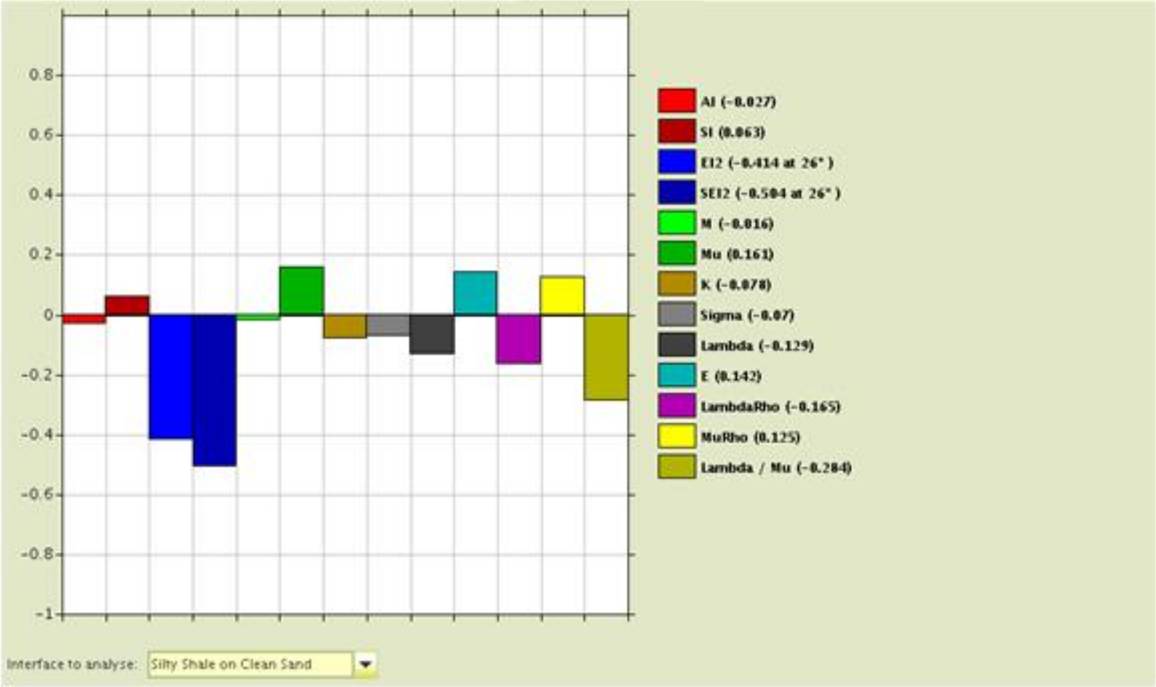

Interface to analyse: Silty Shale on Clean Sand

Figure 4. Elastic contrast analyser for silty-shale on clean sand. Each colour bar represents elastic property contrast at the interface of the two layers

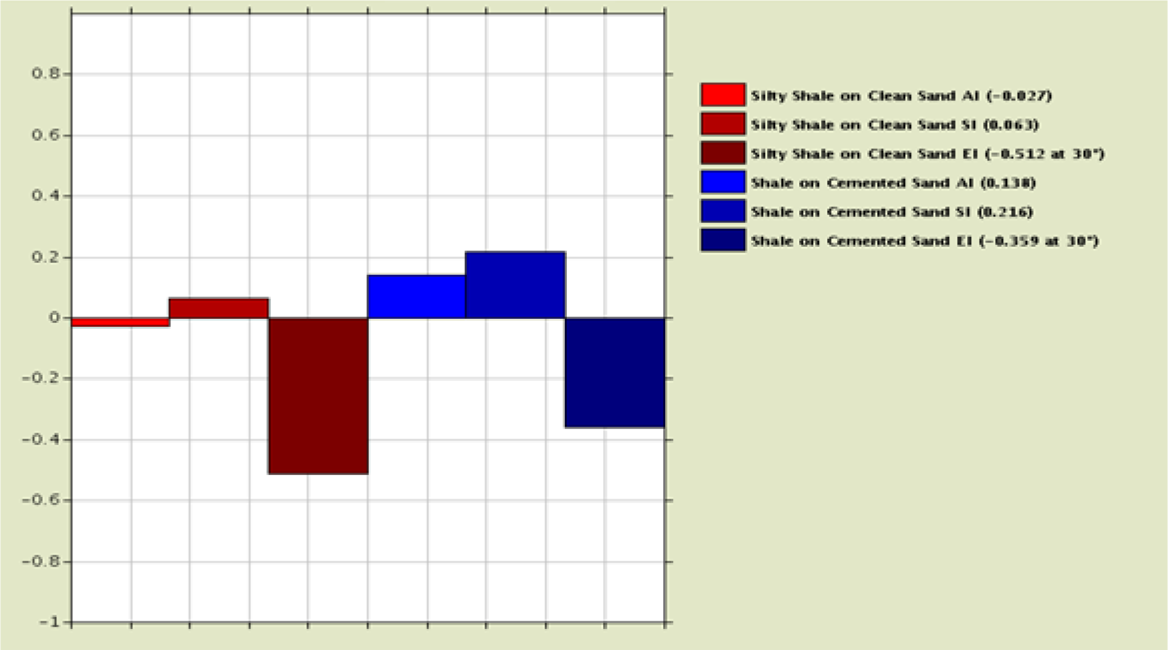

Figure 5. AI, SI and EI contrast analyser for silty-shale on clean sand and cemented sandstone capped by shale. Each colour bar represents elastic property contrast at the interface of the two layers.

Super Gathers formation

Super gathers formation, an important procedure in the AVO analysis on the 2D data is the process of forming average CDPs to enhance the signal-to-noise ratio. The averaging is done by collecting adjacent CDPs and adding them together. In Hampson Russell's AVO 'number of offsets' specifies what each output CDP will have. The number of offsets 35 was used. This means 35 traces will be distributed through the entire offset range, regardless of how many traces there were in the input CDP (number of input offsets was 30). The size of rolling window 5 was used. This means 5 adjacent CDPs will be averaged to produce each output CDP. The super gathers formed (Figure 6) appear cleaner than the original.

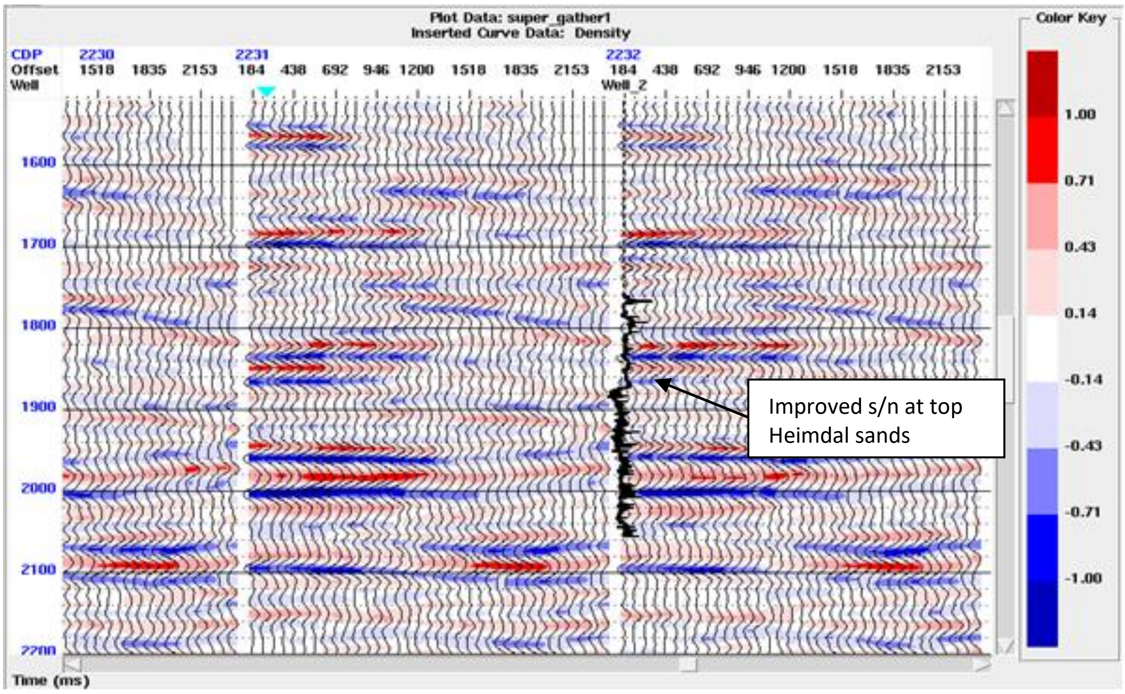

Figure 6. Supergathers formed to enhance signal to noise ratio of the 2D line of CDP gathers. The inserted log is a density log from well 2. The colour bar represents reflectivity. Parameters used are 35 offsets and rolling window of size 5.

AVO attributes volume formation

To produce attribute volume we need to specify the velocity information to be used in calculating the incidence angle. Corrected sonic log from the database was used. The AVO attribute produced (Figure 8) is a plot of the product of intercept and gradient, A*B. Hampson Russell's AVO can allow all the attribute combinations calculated to be seen.

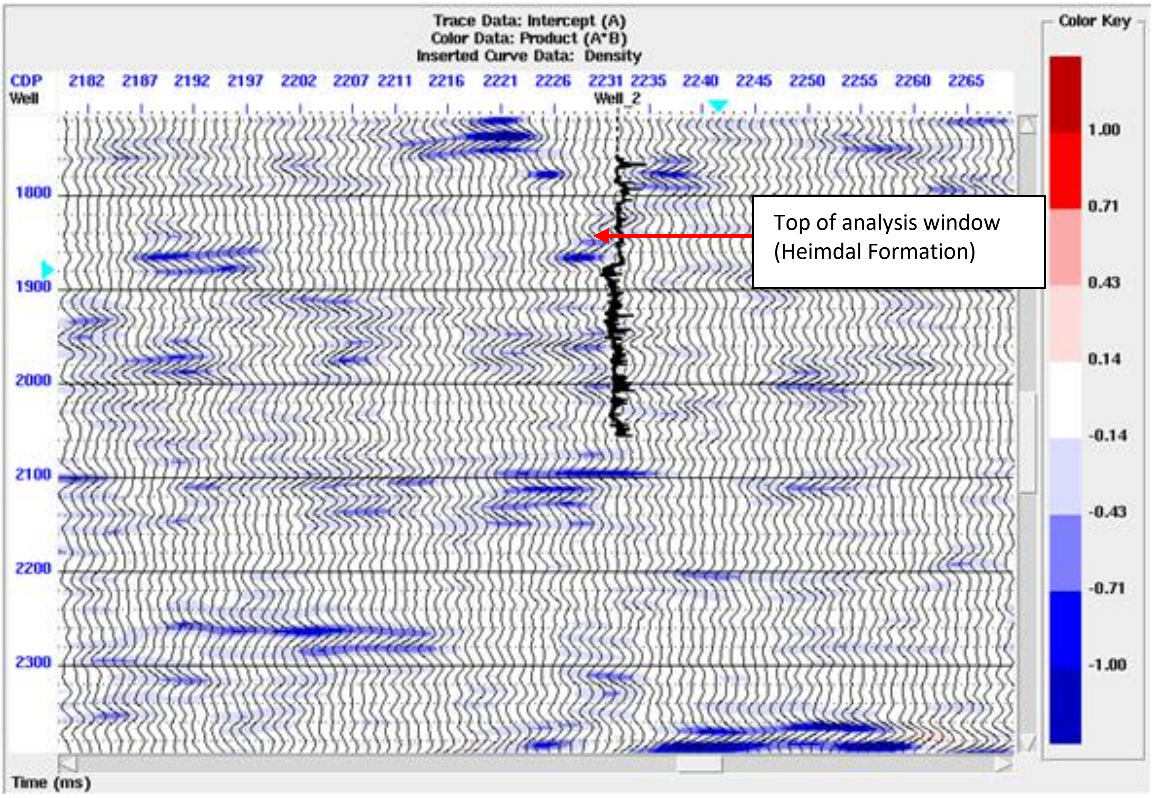

*Figure 7. AVO attribute volume plotted as a product of intercept and gradient A*B. The horizontal axis is the CDP number and the vertical axis is the two-way time in ms. The colour bar represents reflectivity. Annotated is the analysis window for cross plot analysis.*

Cross plotting

The 2D AVO analysis applied to the data set is to cross plot the calculated Intercept and Gradient (Figure 7). The parameters used include: about 80 traces selected as the presumed anomaly region, a constant time window of size 100 ms, centred at the time of 1867 ms (arrowed) representing top of Heimdal Formation sand (unconsolidated sand). In addition, only the peaks and troughs of the data were plotted in order to reduce the volume. Offsets variations in amplitude for reflecting interfaces are represented as single points in cross-plots of intercept and gradient. The advantage of this type of plot is that a great deal of information can be presented and trends can be observed in the data that would be impossible to see with a standard offset versus amplitude cross- plot. The cross-plot is an ideal way examining differences in AVO responses that may be related to lithologic or fluid type variations.

Using intercept gradient data volumes and small target specific window where VpVs are nearly invariant, a background trend can often be determined which define the wet-sand shale interfaces and other similar lithologies. Gradient intercept pairs lying off the trend are considered anomalous. The horizon cross-plot targets the top Heimdal Formation sand, presumed to be reservoir of interest (Figure 8). The cross-plot shows a large background trend passing through the origin with no any significant deviation. It is evident that the sands plotted along the background trend. Studies by Avseth *et al*., (2005) stated that this type of anomaly (AVO class 2), representing sands saturated with hydrocarbons that have very weak zero-offset with the cap-rock, can show great overlap with the background trend especially if they are relatively deep. Hence the intercept-gradient cross plot is unable to differentiate the sands anomaly from the background trend.

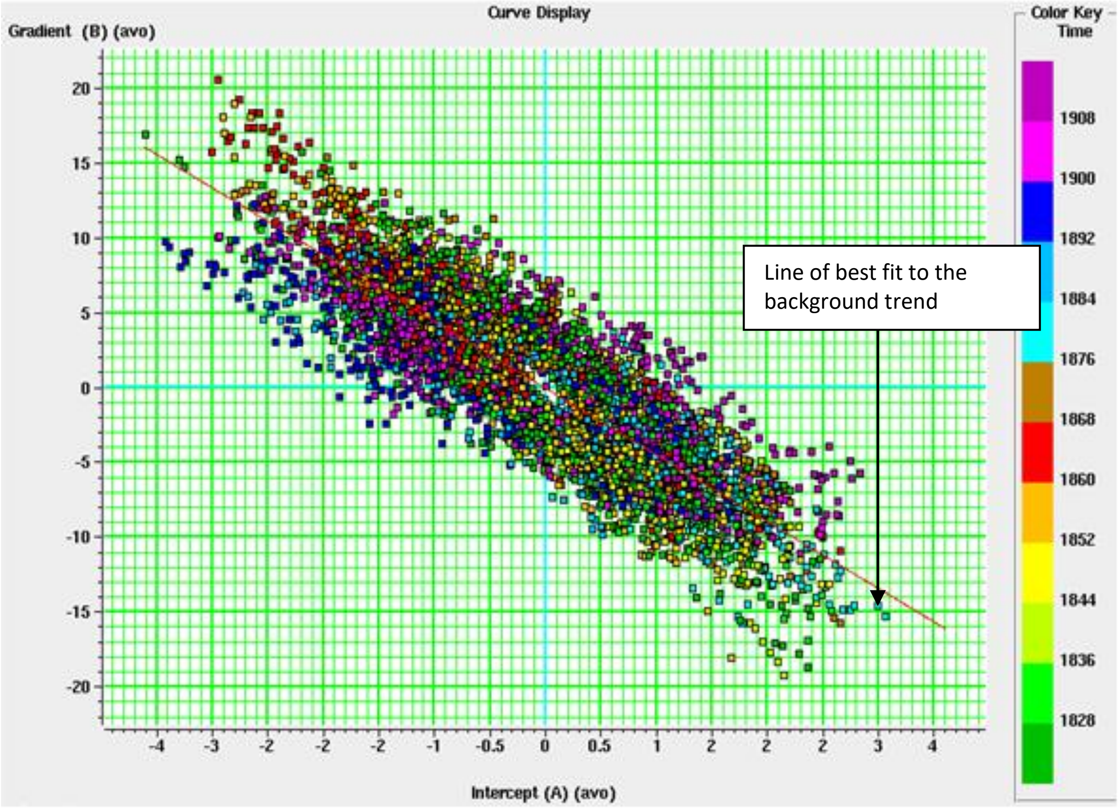

Line of best fit to the background trend

Figure 8. Gradient versus Intercept cross-plot of the top Heimdal Formation sand (Top clean sand) at constant time of 1867 ms using a 100ms time-window centred on the slice.

V. Conclusions

This study evaluated the application of Amplitude Variation with Offset (AVO) analysis for reservoir characterization of the Paleocene Heimdal Formation in the northern North Sea. The results demonstrate that AVO analysis provides valuable information on lithological variability and pore-fluid distribution, thereby reducing the uncertainty associated with conventional post-stack seismic interpretation.

The AVO modelling showed that unconsolidated clean sandstone exhibits relatively weak amplitude variations with increasing offset because of the small acoustic impedance contrast between the reservoir and the overlying silty shale. In contrast, cemented sandstone produced stronger amplitude anomalies resulting from higher elastic impedance contrasts associated with quartz cementation. These findings indicate that lithological variations exert a major control on AVO signatures in the Heimdal Formation and should be carefully considered during seismic interpretation.

Analysis of AVO intercept and gradient attributes demonstrated that the combined use of these parameters provides a reliable means of distinguishing sandstone from shale and identifying variations in reservoir quality. Supergather processing further improved the quality of prestack seismic gathers by enhancing the signal-to-noise ratio, resulting in more stable estimation of AVO attributes and greater confidence in interpretation.

References

[1]. Avseth, P., Mukerji, T., Jørstad A., Mavko G., And Veggeland, T., (2001a). Seismic Reservoir Mapping From 3-D AVO In A North Sea Turbidite System. Geophysics, Vol. 66, 1157-1176.
[2]. Avseth, P., Mukerji, T., Mavko, G., And Tyssekvam, J. A., (2001b). Rock Physics And AVO Analysis For Lithofacies And Pore Fluid Prediction In A North Sea Oil Field. The Leading Edge, 20, 429-434.
[3]. Avseth, P., Mukerji, T. And Mavko, G. (2009). Quantitative Seismic Interpretation. Cambridge University Press.
[4]. Mavko, G., Mukerji, T., And Avseth, P. (2005). Quantitative Seismic Interpretation: Applying Rock Physics Tools To Reduce Interpretation Risk. Cambridge University Press.
[5]. Batzle, E. G. And Wang, Z. (1992). Seismic Properties Of Pore Fluids. Geophysics, 57(11), 1396–1408.
[6]. Castagna, J.P., And Backus, M. M.,(2000) Offset-Dependant Reflectivity—Theory And Practice Of AVO Analysis. Investigations In Geophysics Series, Volume 8, Society Of Exploration Geophysicists, 3-14
[7]. Cayley, G. T., (1987) Hydrocarbon Migration In The Central North Sea. In Petroleum Geology Of North West Europe. Brookes, J, And Glennie, K. W., (Editors). (London: Graham And Trotman), 549-555.
[8]. Eissa, M. A., Pfeiffer, J., And Ortega, A. P., (2009) Seismic Petrophysical Analysis For Thin Sandstones Reservoirs In Colombia's Guajira Basin. The Leading Edge, 28, 640-647.

[9]. Gassmann. F., (1951). Über Die Elastizität Poröser Medien. Vierteljahrsschrift Der Naturforschenden Gesellschaft In Zürich, 96, 1–23.

[10]. Greenberg, M. L., & Castagna, J. P., (1992). Shear-Wave Velocity Estimation In Porous Rocks: Theoretical Formulation, Preliminary Verification And Applications. Geophysical Prospecting, 40(2), 195–209.

[11]. Hampson Russell., 1999, STRATA/UNIX Stratigraphic Analysis And Inversion Manual.

[12]. Dvorkin, J., Mavko, G., And Mukerji, T., (2009). The Rock Physics Handbook (2nd Ed.). Cambridge University Press.

[13]. Jordt, H., Feliede, I. E., Bjolykke, K., And Ibrahim, M. T., (2003), Cenozoic Sequence Stratigraphy Of The Central And Northern North Sea Basin: Tectonic Development, Sediment Distribution And Provenance Areas. Marine And Petroleum Geology. Vol. 12, Issue 8, 845-879.

[14]. Knox, R.W.O'B., And Holloway, S., (1992). Paleogene Of The Central Northern North Sea. Lithostratigraphic Nomenclature Of The UK North Sea, Vol. 1. Knox R.W.O'B., And Cordey, W.G., (Editors). Nottingham British Geological Survey.

[15]. Mukerji, T., Avseth, P., Mavko, G., Takahashi, I., & González, E. (2001). Statistical Rock Physics: Combining Rock Physics, Information Theory And Geostatistics To Reduce Uncertainty In Seismic Reservoir Characterization. The Leading Edge, 20(3), 313–319.

[16]. Neil, J. E., (1996). A Summary Of Paleogene Sequence Stratigraphy In Northwest Europe And The North Sea. 15-42 In Correlation Of The Early Paleozoic In Northwest Europe. Knox, R W O'B, Corfield, R. M., And Dunay, R. E., (Editors). Special Publication Of Geological Society Of London, No. 101.

[17]. O'Connor, S. J., And Walker, D., 1993, Paleocene Reservoirs Of The Everest Trend. 14-160 In Petroleum Geology Of Northwest Europe: Proceedings Of The 4th Conference. Parker, J. R., (Editor). (London: The Geological Society Of London.)

[18]. Rutherford, S. R., And Williams, R. H., 1989, Amplitude-Versus-Offset Variations In Gas Sands. Geophysics, 54, 609-814.

[19]. Seirra, J.,Campos, H.,Bonilla, M., Paz, D., Marin, W., Cardinez, S., And Joseph, D., 2009, Seismic Multiattribute Integration For Prospect Generation In South Main Saldado Field, Gulf Of Paria, Trinidad And Tobago.The Leading Edge, 28, 684-689.

[20]. Shuey, R. T., 1985, A Simplification Of Zoeppritz Equations. Geophysics, 50, 609-814.

[21]. Whyatt, J., Bowen J. M., And Rhodes D. N., 1991: Successful Application Of A Development Geoseismic Model In North Sea Exploration, *Geological Society, London, Special Publications*. V 67, 283